Asian Journal of Chemistry; Vol. 34, No. 5 (2022), 1125-1133

ASIAN JOURNAL OF CHEMISTRY

https://doi.org/10.14233/ajchem.2022.23615

Complexes of Organyltellurium(IV) with Neutral [N,O] Donor Schiff Base Derived from Substituted Furfuraldehyde and Toluidine: Synthesis, Structural Characterization, Computational Studies and Biological Evaluation

NIDHI ANTIL, MANISH KUMAR, K.K. VERMA and SAPANA GARG*

Department of Chemistry, Maharshi Dayanand University, Rohtak-124001, India

*Corresponding author: E-mail: sapanagarg1511@gmail.com

Received: 12 November 2021; *Accepted*: 31 December 2021; *Published online*: 20 April 2022; AJC-20762

Organyltellurium(IV) complexes of Schiff base (MeFPT = 4-methyl-N-((5-methylfuran-2-yl)methylene)aniline) derived from condensation reaction of 5-methyl furan-2-carboxaldehyde with *p*-toluidine having formula of type MeFPT·$RTeCl_3$ and MeFPT·R_2TeCl_2 (R = 4-hydroxyphenyl, 4-methoxyphenyl or 3-methyl-4-hydroxyphenyl) were reported. These complexes have been characterized by elemental analysis, IR, ^1H NMR, ^{13}C NMR, UV-Vis, DFT, molecular modelling and mass spectra. The experimental data demonstrated that formed Schiff base complexes behaved as bidentate ligand with R_1TeCl_3 and R_2TeCl_2 chelated by neutral N and O atoms having distorted octahedral stereochemistry in all organyltellurium(IV) complexes. Schiff base and its organyltellurium(IV) complexes exhibited considerable biological activity. The antibacterial and antifungal activity have been carried out and the results were compared with some known antibiotics.

Keywords: Schiff base, 5-Methylfuran-2-carboxaldehyde, 4-Toluidine, Organyltellurium(IV) complexes, Biological activity.

INTRODUCTION

The Schiff bases are considered as organic bioactive ligands, which form complexes with metals and metalloids. They are synthesized *via* a condensation reaction between primary amine groups and aldehydes/ketones, known as imine (C=N) or azomethine (CH=N) [1] groups containing nitrogen analogues of aldehydes/ketones where the carbonyl group has been substituted by an imine or azomethine group. Schiff base ligands comprising mainly O,N,S donor atoms are being explored as an important class of ligands because they can coordinate and stabilize a wide range of metal ions in various oxidation states [2,3]. Schiff Bases have been found to have a broad range of biological [4] behaviour, including antimicrobial [5-8], antiviral [9], antitumour, antibacterial, fungicidal and anticarcinogenic properties [10-13]. Schiff Base ligands also used as optical and electrode sensors [14] as well as in various chromatographic method to enhance selectivity and sensitivity [15-17]. They are used also as intermediate in organic synthesis, dyes and pigments and as polymer stabilizers [18]. Studies associated to metal based drugs are both encouraging and have intense interest in biology and chemistry. Organic bioactive heterocyclic Schiff bases and associated metal complexes synthesized by reactions with metal chlorides including nitrogen and oxygen donor atoms have been acknowledged in biomedical applications, supramolecular chemistry and material sciences [19].

The furan ring, as a component of the Schiff base ligand, has long been investigated and a source of attraction. Schiff bases produced from furaldehyde have nitrification inhibitory properties [20] and antimicrobial action. Furthermore, due of its numerous applications, such as emitting materials for organic light emitting diodes, light harvesting materials for photocatalysis and fluorescence sensors for organic and inorganic analytes [21], furaldehyde based ligands are also utilized as luminous substances. Apart from other various aspects, the interest of the scientists is very much in knowing their varied biological activities. So, in this work, we have focused on the synthesis of Schiff base ligand and its six metal complexes with organyltellurium compounds [22-26], with the structural characterization, computational studies and antimicrobial properties.

EXPERIMENTAL

Analytical reagent grade chemicals and solvents were used throughout the synthesis. *p*-Toluidine and 5-methyl furan-2-carboxaldehyde were obtained from Sigma-Aldrich, USA in extremely pure form and utilized without additional purification. For the synthesis of metal complexes, tellurium metal chloride (Sigma-Aldrich, USA) was used. Organyltellurium trichloride and diorganyl tellurium dichloride were synthesized in an inert atmosphere of nitrogen by reacting $TeCl_4$ with phenol, anisole and cresol. To perform biological activities and to synthesize metal complexes, as well as solvents, were employed and standard procedure [27,28] was used for drying purposes, where needed.

Physical measurements: A Thermo Finnigan CHNS analyzer was used to perform elemental analysis of the prepared compounds. Melting points of the synthesized ligand and their complexes were determined using open capillaries and are not corrected. Fourier transform infrared (FTIR) spectra of compounds were obtained on a NICOLET iS50 that had been operated as a KBr disc in the range 4000-400 cm^{-1}. ^{13}C NMR and ^{1}H NMR spectra were plotted at room temperature on a Bruker advance III 400 MHz spectrometer employing DMSO-d_6 as the solvent or δ values relative to deuterated DMSO. The SCIEX Triple TOF5600 mass spectrometer was used to record the mass spectra of the ligand and its metal complexes. In DMSO/ethanol, the electronic absorption was assessed using a Shimadzu UV-3600 plus in DMSO/ethanol. The molar conductance was evaluated using a MICROSIL conductometer at 25 ± 1 ºC in solution of the ligand and its metal complexes in DMSO (10^{-3} M).

Synthesis of Schiff base ligand (MeFPT): *p*-Toluidine (3.27 g, 30 mmol) was dissolved in ~ 25 mL absolute ethanol and subsequently added to a magnetically stirred solution of 5-methyl furan-2-carboxaldehyde (2.98 g, 30 mmol). After 4-5 h of refluxing, the mixture was cooled to room temperature. The solution was then condensed to half its original volume. The resulting product was filtered, washed multiple times and recrystallized from ethanol (**Scheme-I**). Colour: orange red; m.w.: 199.10 g/mol; m.p.: 107-110 ºC; yield: 82.34%. ^{1}H NMR (400 MHz, DMSO-d_6) δ ppm: 8.36 (s, 1H, CH=N), 6.49-7.57 (m, 4H, Ar-H), 6.25-7.57 (d, 2H, furan ring), 2.52 (s, 3H, CH_3), 2.38 (s, 3H of furanyl ring). ^{13}C NMR (400 MHz, DMSO-d_6) δ ppm: 142.05 (C2), 116.39 (C3), 113.37 (C4), 125.16 (C5), 146.36 (C7), 131.37 (C8), 134.38 (C9), (C13), 134.31 (C10), (C12), 131.37 (C11), 27.39 (C6), 26.49 (C14). Elemental analysis of $C_{13}H_{13}NO$ calcd. (found) %: C, 78.36 (78.42); H, 6.58 (6.64); N, 7.03 (7.00).

Synthesis of organyltellurium(IV) compounds: As reported in the literature, $TeCl_4$ reacting with hydroxybenzene, methoxybenzene and 2-methyl phenol in 1:1 and 1:2 molar ratio led to the formation of $RTeCl_3$ and R_2TeCl_2.

$$RH + TeCl_4 \longrightarrow RTeCl_3$$

$$2RH + TeCl_4 \longrightarrow R_2TeCl_2$$

Synthesis of organyltellurium(IV) complexes ($RTeCl_3\cdot$MeFPT and $R_2TeCl_2\cdot$MeFPT): The metal complexes were synthesized by stirring a solution of ligand (1 mmol) in 20 mL methanol under warm conditions and then adding a solution of $RTeCl_3$/R_2TeCl_2 (1 mmol) in 20 mL methanol dropwise while stirring continuously. The mixture solution was then refluxed at 80 ºC for 4 h while stirring. The complexes were filtered out of the supernatant liquid, washed with methanol and dried on anhydrous calcium chloride (**Scheme-II**).

$C_{19}H_{18}Cl_3NO_2Te$ (1a): Colour: brown; yield 82%; m.p.: 150 ºC; Elemental analysis: calcd. (found) %: C, 43.36 (43.31); H, 3.45 (3.49); N, 2.66 (2.74); Te, 24.24 (24.06); Cl, 20.21 (20.15). IR (KBr, selected bands, cm^{-1}): 3361 (b, O-H *str.*), 1608 (s, C=N), 1273 (s, C-O-C), 287 (Te-N), 509 (Te-O). ^{1}H NMR (400 MHz, DMSO-d_6) δ ppm: 9.56 (s, 1H, Ar-OH), 6.01-7.86 (m, 10H, Ar-H of furan and benzene ring), 8.83 (s, 1H, C=N), 2.52 (s, 3H, CH_3 of furan), 2.36 (s, 3H, CH_3); ^{13}C NMR: 147.63 (C2), 105.34 (C3), 104.39 (C4), 143.71 (C5), 16.98 (C6), 167.66 (C7), 146.01 (C8), 119.17 (C9, C13), 134.13 (C10, C12), 140.95 (C11), 22.45 (C14), 145.23 (C15), 136.67 (C16, C20), 115.81 (C17, C19), 161.74 (C18).

$C_{20}H_{20}Cl_3NO_2Te$ (1b): Colour: brown red; yield 85.32%; m.p.: 162 °C; Elemental analysis: calcd. (found) %: C, 44.46 (44.28); H, 3.73 (3.56); N, 2.59 (2.57); Te, 23.61 (23.57); Cl, 19.68 (19.62); IR (KBr, selected bands, cm^{-1}): 1602 (s, C=N), 1227 (s, C-O-C), 290 (Te-N), 513 (Te-O); ^{1}H NMR (400 MHz, DMSO-d_6) δ ppm: 3.83 (s, 3H, OCH_3 group), 6.85-7.69 (m, 16H, Ar-H of furan and benzene ring), 8.37-8.67 (s, 1H, C=N), 2.30 (s, 3H, CH_3 group of furan ring), 2.34 (s, 3H, CH_3 group). ^{13}C NMR: 149.98 (C2), 103.07 (C3), 107.21 (C4), 141.01 (C5), 15.79 (C6), 163.33 (C7), 160.67 (C8), 118.38 (C9, C13), 132.40 (C10, C12), 141.62 (C11), 21.57 (C14), 144.01 (C15), 136.20 (C16, C20), 123.75 (C17, C19), 160.16 (C18), 55.79 (C21).

$C_{20}H_{20}Cl_3NO_3Te$ (1c): Colour: yellow; yield 82.98%; m.p.: 118 ºC; Elemental analysis: calcd. (found) %: C, 44.46 (44.31); H, 3.73 (3.74); N, 2.59 (2.46); Te, 23.61 (23.35); Cl, 19.68 (19.86); IR (KBr, selected bands, cm^{-1}): 2937 (b, O-H *str.*), 1617 (s, C=N), 1213 (s, C-O-C), 286 (Te-N), 510 (Te-O); ^{1}H NMR (400 MHz, DMSO-d_6) δ ppm: 9.53 (s, 3H, OH group), 6.91-7.88 (m, 16H, Ar-H of furan and benzene ring), 8.37-8.67 (s, 1H, C=N), 2.30 (s, 3H, CH_3 group of furan ring), 2.34 (s, 3H, CH_3 group); ^{13}C NMR: 149.98 (C2), 103.07 (C3), 107.21 (C4), 141.01 (C5), 15.79 (C6), 163.33 (C7), 160.67 (C8),

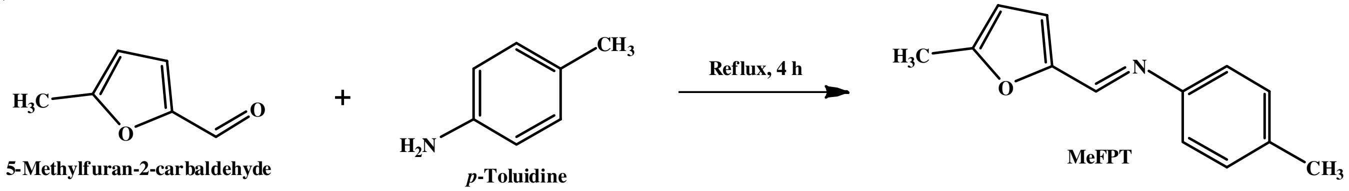

Scheme-I: Synthesis of Schiff base ligand (MeFPT)

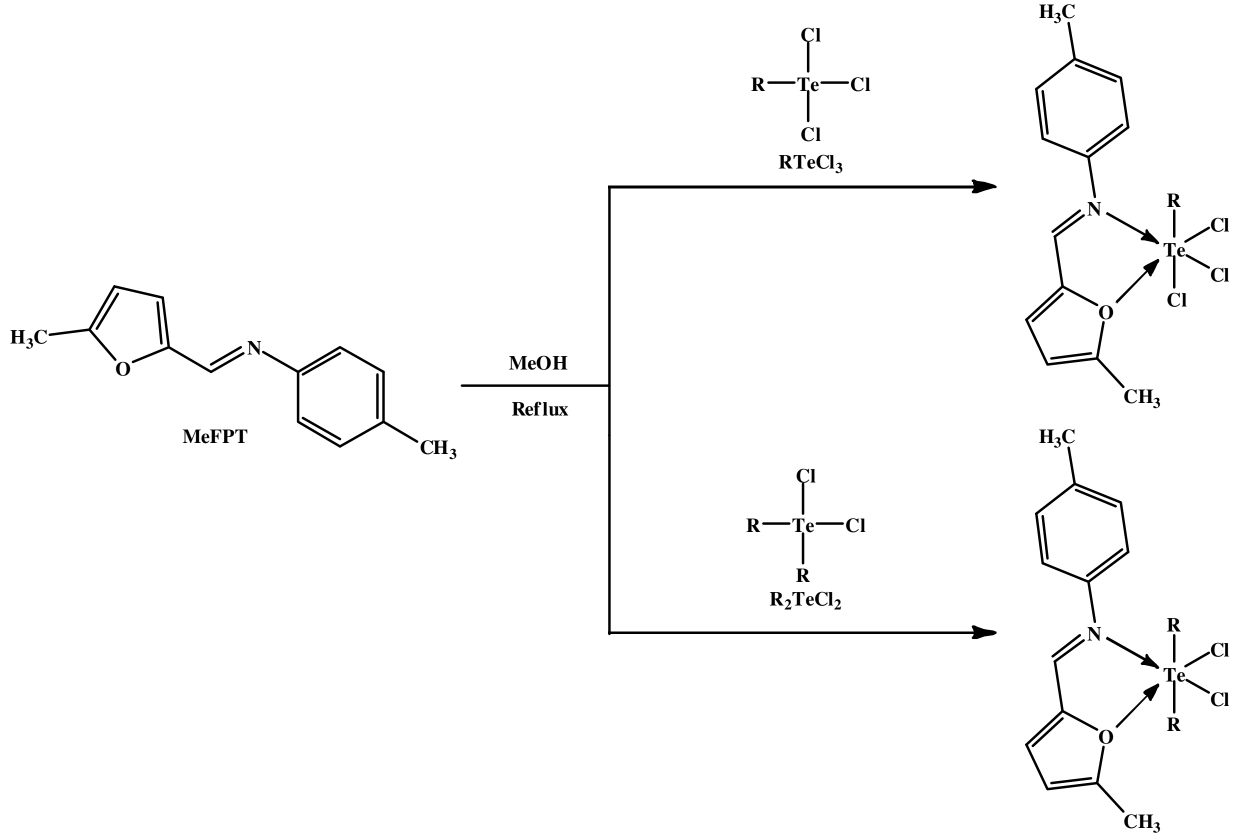

Scheme-II: Synthesis of $RTeCl_3 \cdot MeFPT$ and $R_2TeCl_2 \cdot MeFPT$

118.38 (C9, C13), 132.40 (C10, C12), 141.62 (C11), 21.57 (C14), 144.01 (C15), 136.20 (C16, C20), 123.75 (C17, C19), 160.16 (C18), 55.79 (C21).

$C_{25}H_{23}Cl_2NO_3Te$ (1d): Colour: brown; yield 78.41%; m.p.: 83.77 ºC; Elemental analysis: calcd. (found) %: C, 51.42 (51.35); H, 3.97 (4.05); N, 2.40 (2.33); Te, 21.85 (21.23); Cl, 12.14 (12.37); IR (KBr, selected bands, cm^{-1}): 3317 (b, O-H *str.*), 1593 (s, C=N), 1217 (s, C-O-C), 292 (Te-N), 512 (Te-O); ^{1}H NMR (400 MHz, DMSO-d_6) δ ppm: 3.83 (s, 2H, Ar-OH), 6.08-7.54 (m, 20H, Ar-H of furan and benzene ring), 8.77 (s, 1H, C=N), 2.34 (s, 3H, CH_3 group of furan ring), 2.47 (s, 3H, CH_3 group); ^{13}C NMR: 144.92 (C2), 106.27 (C3), 110.71 (C4), 144.31 (C5), 14.49 (C6), 157.03 (C7), 144.87 (C8), 121.68 (C9, C13), 129.40 (C10, C12), 136.92 (C11), 21.77 (C14), 128.31 (C15), 136.70 (C16, C20), 115.05 (C17, C19), 158.76 (C18), 128.69 (C21), 135.24 (C22, C26), 115.38 (C23, 25), 157.91 (C24).

$C_{27}H_{27}Cl_2NO_3Te$ (1e): Colour: dark brown; yield 87.41%; m.p.: 98.7 ºC; Elemental analysis: calcd. (found) %: C, 52.99 (52.84); H, 4.45 (4.43); N, 2.29 (2.33); Te, 20.85 (19.29); Cl, 11.59 (12.17); IR (KBr, selected bands, cm^{-1}): 1612 (s, C=N), 1176 (s, C-O-C), 293 (Te-N), 506 (Te-O); ^{1}H NMR (400 MHz, DMSO-d_6) δ ppm: 3.79 (s, 3H, OCH_3 group), 6.21-7.38 (m, 20H, Ar-H of furan and benzene ring), 8.67 (s, 1H, C=N), 2.27 (s, 3H, CH_3 group of furan ring), 2.54 (s, 3H, CH_3 group); ^{13}C NMR: 155.62 (C2), 107.97 (C3), 110.51 (C4), 152.71 (C5), 15.64 (C6), 162.73 (C7), 123.77 (C8), 121.04 (C9, C13), 129.31 (C10, C12), 123.72 (C11), 22.37 (C14), 128.41 (C15), 135.71 (C16, C20), 123.75 (C17, C19), 147.66 (C18), 55.79 (C21), 127.94 (C22), 136.38 (C23, 27), 124.31 (C24, C26), 146.18 (C25), 55.36 (C28).

$C_{27}H_{27}Cl_2NO_3Te$ (1f): colour: brown; yield 82.27%; m.p.: 103 ºC; Elemental analysis: calcd. (found) %: C, 52.99 (52.84); H, 4.45 (4.43); N, 2.29 (2.33); Te, 20.85 (19.29); Cl, 11.59 (12.17); IR (KBr, selected bands, cm^{-1}): 3348 (b, O-H *str.*), 1606 (s, C=N), 1221 (s, C-O-C), 289 (Te-N), 511 (Te-O); ^{1}H NMR (400 MHz, DMSO-d_6) δ ppm): 10.02 (s, 1H, Ar-OH), 6.11-7.86 (m, 20H, Ar-H of furan and benzene ring), 8.55 (s, 1H, C=N), 2.37 (s, 3H, CH_3 group of furan ring), 2.51 (s, 3H, CH_3 group); ^{13}C NMR: 144.82 (C2), 107.37 (C3), 109.71 (C4), 143.71 (C5), 13.74 (C6), 163.73 (C7), 143.17 (C8), 120.74 (C9, C13), 131.21 (C10, C12), 137.22 (C11), 21.67 (C14), 128.71 (C15), 131.81 (C16), 130.25 (C17), 154.16 (C18), 114.73 (C19), 134.83 (C20), 15.19 (C21), 128.34 (C22), 131.28 (C23), 128.41 (C24), 155.21 (C25), 114.88 (C26), 132.66 (C27), 15.46 (C28).

Computational method: Orca 4.0 program package has been used to represent all the DFT computations. Molecular modelling has been employed for the optimizations of structures. DFT functional is renowned for the predictions of energies of molecular complexes using def2-SVP basis sets for the Te(IV) center and other organic elements (C, H, O and N), respectively.

***in vitro* Antimicrobial activity:** The ligand (MeFPT) and its organyltellurium(IV) complexes (**1a-f**) were assayed against fungal strains (*A. clavatus* MTCC 1323, *C. albicans* MTCC 227, *A. niger* MTCC 282), Gram-positive bacterial strains (*S. pyogenes* MTCC 442, *S. aureus* MTCC 96) and Gram-negative bacterial strains (*E. coli* MTCC 443, *P. aerugenosa* MTCC 1688). The Institute of Microbial Technology in Chandigarh , India provided the bacterial strains. By using the broth dilution method and the agar well-diffusion method, we were able to compare their antifungal and antibacterial efficacy. DMSO was employed as a diluent to achieve the necessary medication concentration for testing on typical bacterial strains. The samples were incubated for 24 to 30 h at 37 ºC.

RESULTS AND DISCUSSION

All the tellurium metalloid complexes containing Schiff base were synthesized by using refluxing method. The metal complexes are solid, air stable and soluble in ethanol, methanol, DMSO and DMF. The change in colour from ligand to metal complexes is in support of metal-ligand interaction, which is further proved by conductivity. Using elemental analysis, IR, UV-Vis, NMR, DFT the structural features of organyltellurium (IV) complexes were elucidated.

Conductance studies: The molar conductivity [29-31] values in ohm^{-1} cm^{2} mol^{-1} of all the organyltellurium(IV) complexes (**1a-f**) in DMSO 10^{-3} M solution are shown in Table-1. This suggests their non-electrolytic nature of synthesized compounds.

Mass spectra: The structure of the Schiff base ligand and its organyltellurium complexes as well as their molar weight were analyzed *via* mass spectroscopy. However, it also fortifies the proposed empirical formula of ligand. The molecular ion peaks for ligand were observed at 200 *m/z*, which corresponded to the molecular weight of ligand. All the data of molecular ion peak, base peak are in accordance with the structure of ligand. The mass spectral analysis results of tellurium complexes (**1a-f**) reveal molecular ion peaks *m/z* at 528, 540, 541, 583, 613, 614 correspond to the molecular weights of these complexes. The mass spectra of MeFPT ligand and organyltellurium(IV) complex (**1a**) is shown in Fig. 1.

TABLE-1
MOLAR CONDUCTANCE VALUES OF THE SYNTHESIZED ORGANYLTELLURIUM(IV) COMPLEXES

Compound	Molar conductance (Ohm^{-1} cm^{2} mol^{-1})	Compound	Molar conductance (Ohm^{-1} cm^{2} mol^{-1})
1a	29.08	**1d**	49.52
1b	25.42	**1e**	41.90
1c	26.44	**1f**	46.78

IR spectra: The IR spectra of the ligand and its organyltellurium(IV) complexes were analyzed using bands in the 4000-400 cm^{-1} range (Fig. 2) to obtain the coordination sites. The stretching vibrations C-O-C, C=N, N-Te, O-Te were analyzed for the structural confirmation of ligand and their respective complexes. Table-2 lists the key infrared bands of Schiff Base ligand and its organyltellurium(IV) complexes. The IR spectrum in KBr disc of ligand has an intense absorbtion band at 1631 cm^{-1} ascribed to the stretching vibration (C=N) and shifted to lower wavenumber [32,33] due to complex formation, which indicating the coordination of Schiff base to the tellurium metal ion [34-36] *via* azomethine-N atom. Due to the (C=O) stretching frequency [37], both the ligand and its organyltellurium metal complexes displayed no band at 1735 cm^{-1}. In ligand, a medium intensity absorption band due to the (C-O-C) [38] stretching vibration of furan was observed at 1291 cm^{-1}. These bands were

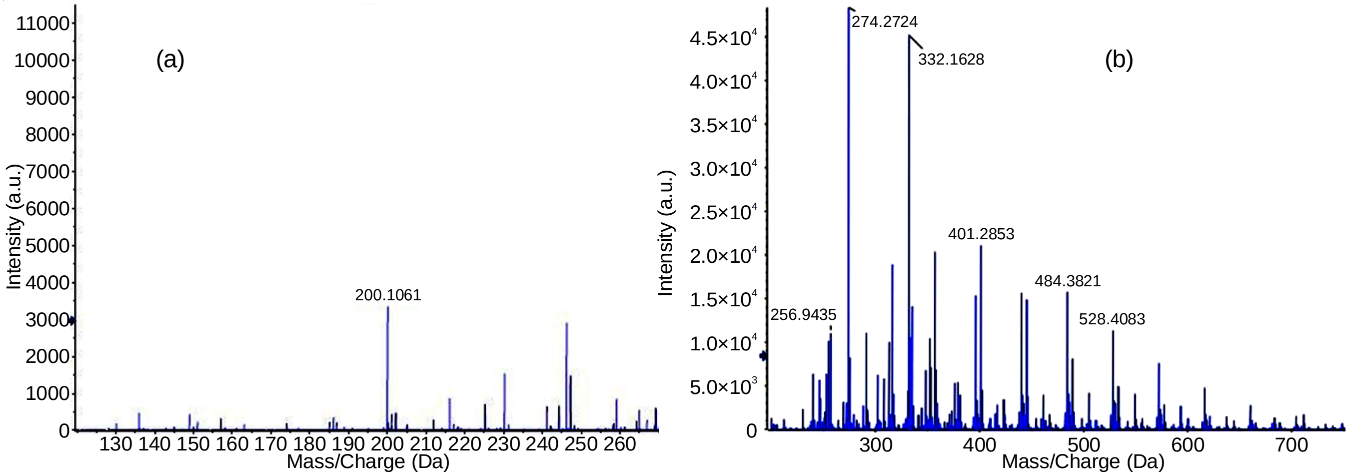

Fig. 1. Mass spectrum of Schiff base (a) ligand (MeFPT) and (b) organyltellurium(IV)complex (**1a**)

TABLE-2
IR SPECTRAL DATA (cm^{-1}) OF (MeFPT) LIGAND AND ITS ORGANYLTELLURIUM(IV) COMPLEXES

Compound	ν(O-H)	ν(C-H) stretching	ν(C-H) aromatic stretching	ν(C-O-C)	ν(C=N)	ν(Te-N)	ν(Te-O)
MeFPT	–	2926	3054	1291	1631	–	–
1a	3361	2938	3058	1273	1608	287	509
1b	–	2931	3064	1227	1602	290	513
1c	3324	2937	3061	1213	1617	286	510
1d	3317	2936	3057	1217	1593	292	512
1e	–	2923	3051	1176	1612	293	506
1f	3348	2939	3063	1221	1606	289	511

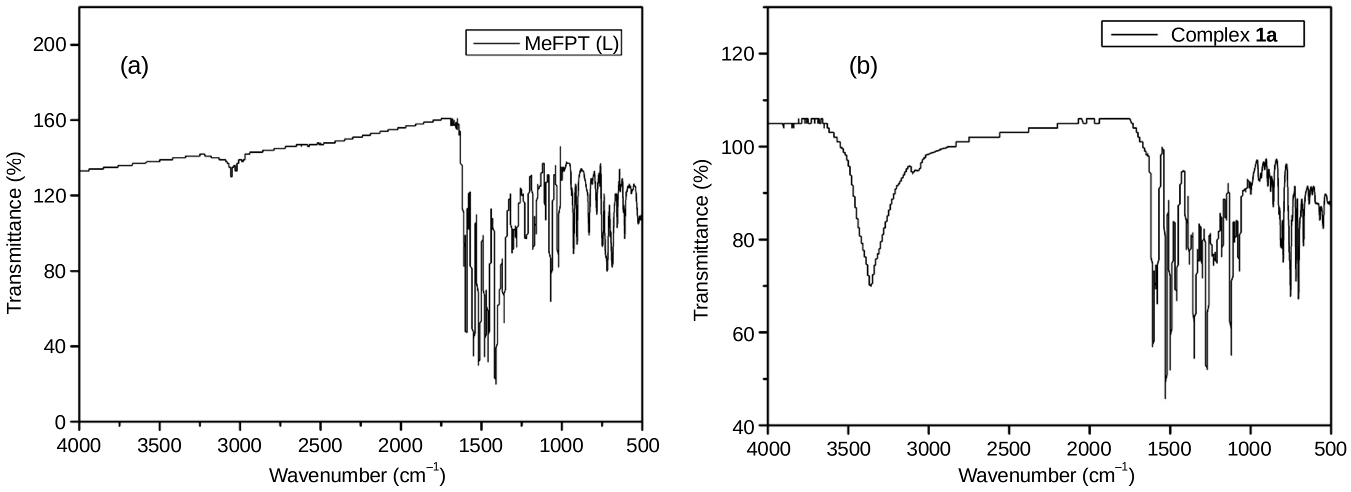

Fig. 2. FT-IR spectrum of (a) ligand (MeFPT) and (b) organyltellurium(IV) complex (**1a**)

moved towards the lower wavenumber region in all corresponding metal complexes indicating that the furan moiety is coordinated through oxygen. The formation of the complexes was confirmed by the appearance of a new band in the spectra of the complexes in the range 292-287 cm^{-1} and 513-506 cm^{-1}, which was assigned to the (Te-N) and (Te-O) [39-41] stretching vibrations, respectively. The study demonstrates that Schiff base ligand act as neutral bidentate coordinating *via* O and N atom in complexes having distorted octahedral stereochemistry.

^{1}H NMR spectra: Table-3 lists the chemical shifts of various types of proton in Schiff base ligand and and its organyltellurium(IV) complexes. The azomethine proton were distinguished by a singlet in the δ 8.36 ppm region of the parent ligand. The aromatic and furan ring protons were also shown to be responsible for multiplets in the range 6.25-7.57 ppm in the ligand. Meanwhile, ^{1}H NMR spectra of organyltellurium(IV) complexes showed a signal at 8.37-8.83 ppm for CH=N that was moved to a higher region in contrast to free ligands implying coordination [42] through the azomethine N atom of the ligand. The aromatic and furan ring protons signals were detected as multipl in the range of 6.08-7.88 ppm showing that the oxygen of furan ring [43,44] is involved in organyltellurium(IV) complex coordination.

TABLE-3
^{1}H NMR SPECTRAL DATA OF (MeFPT) LIGAND AND ITS Te(IV) COMPLEXES

Compd.	C-OH	CH=N	CH$_3$	Furan ring protons	Aromatic ring protons
MeFPT	–	8.36	2.38	6.25, 6.26	6.49-7.57
1a	9.56	8.83	2.52	6.91, 7.02	6.91-7.88
1b	–	8.37	2.30	6.80, 6.85	6.79-7.69
1c	9.54	8.46	2.27	6.91, 6.76	6.81-7.88
1d	10.17	8.77	2.34	6.08, 6.98	6.63-7.54
1e	–	8.67	2.27	6.21, 6.99	6.57-7.38
1f	10.02	8.55	2.37	6.91, 6.99	6.88-7.13

^{13}C NMR spectra: The ^{1}H NMR spectral assignments of the new synthesized compounds are also supported by the ^{13}C NMR spectrum and shown in Table-4. The characteristic chemical shifts of the benzene carbon atoms are assigned in the range of 120-170 ppm, similarly the peaks at δ 142.05, δ 116.39, δ 113.37, δ 125.16 ppm values are attributed to the carbons of the furfuryl ring. The ^{13}C NMR analysis shows corresponding peak for imine at δ 146.36-167.66 ppm. The peak at δ 26.49 and δ 21.57-22.45 ppm corresponds to the CH_3 group present in the rings. These results strongly suggest that both N and O atom coordinate to organyltellurium(IV) complexes.

UV-Vis spectra: The UV-Vis electronic spectrum of all the compounds were obtained and showed three distinct absorption bands. In Table-5, the first band will be assigned to intra ligand π-π* transition [45,46] that was observed at 229 nm, while the second characteristic wavelength observed at 292 nm will be assigned to the n-π* transition [47] for the azomethine group (-C=N-), shifts to the red shift and absorbs in the region 292-308 nm in case of complexes. The third band at 424 nm is notable for such charge transfer transition of a azomethine and oxygen atom of a furan ring, after complexation the wavelength shift in range between 434-463 nm, which further indicated the formation of complexes. The significant UV-visible spectral bands of ligand and its organyltellurium(IV) complexes are shown in Fig. 3.

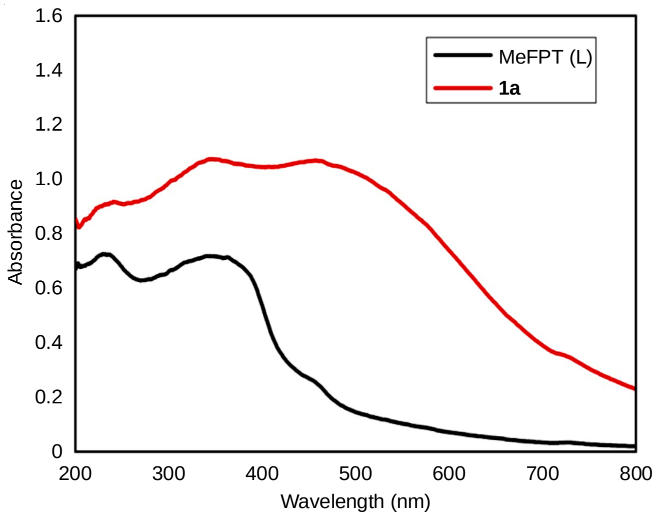

Fig. 3. UV-visible spectrum of (MeFPT) ligand as well as its organyltellurium(IV) complex (**1a**)

TABLE-4
^{13}C NMR SPECTRAL DATA OF (MeFPT) LIGAND AND ITS ORGANYLTELLURIUM(IV) COMPLEXES

Compd.	Chemical shift, δ ppm (DMSO-d_6)		
	CH=N	C-H	Aromatic carbons
L	146.36 (C7)	27.39 (C6), 26.49 (C14)	142.05 (C2), 116.39 (C3), 113.37 (C4), 125.16 (C5), 131.37 (C8), 134.38 (C9), (C13), 134.31 (C10), (C12), 131.37 (C11)
1a	167.66 (C7)	16.98 (C6), 22.45 (C14)	147.63 (C2), 105.34 (C3), 104.39 (C4), 143.71 (C5), 146.01 (C8), 119.17 (C9, C13), 134.13 (C10, C12), 140.95 (C11), 145.23 (C15), 136.67 (C16, C20), 115.81 (C17, C19), 161.74 (C18)
1b	163.33 (C7)	15.79 (C6), 21.57 (C14), 55.79 (C21)	149.98 (C2), 103.07 (C3), 107.21 (C4), 141.01 (C5), 160.67 (C8), 118.38 (C9, C13), 132.40 (C10, C12), 141.62 (C11), 144.01 (C15), 136.20 (C16, C20), 123.75 (C17, C19), 160.16 (C18)
1c	163.33 (C7)	15.79 (C6), 21.57 (C14), 55.79 (C21)	149.98 (C2), 103.07 (C3), 107.21 (C4), 141.01 (C5), 160.67 (C8), 118.38 (C9, C13), 132.40 (C10, C12), 141.62 (C11), 144.01 (C15), 136.20 (C16, C20), 123.75 (C17, C19), 160.16 (C18), 55.79 (C21)
1d	157.03 (C7)	14.49 (C6), 21.77 (C14)	144.92 (C2), 106.27 (C3), 110.71 (C4), 144.31 (C5), 144.87 (C8), 121.68 (C9, C13), 129.40 (C10, C12), 136.92 (C11), 128.31 (C15), 136.70 (C16, C20), 115.05 (C17, C19), 158.76 (C18), 128.69 (C21), 135.24 (C22, C26), 115.38 (C23, 25), 157.91 (C24)
1e	162.73 (C7),	15.64 (C6), 22.37 (C14), 55.79 (C21), 55.36 (C28)	155.62 (C2), 107.97 (C3), 110.51 (C4), 152.71 (C5), 123.77 (C8), 121.04 (C9, C13), 129.31 (C10, C12), 123.72 (C11), 128.41 (C15), 135.71 (C16, C20), 123.75 (C17, C19), 147.66 (C18), 127.94 (C22), 136.38 (C23, 27), 124.31 (C24, C26), 146.18 (C25)
1f	163.73 (C7)	13.74 (C6), 21.67 (C14), 15.19 (C21), 15.46 (C28)	144.82 (C2), 107.37 (C3), 109.71 (C4), 143.71 (C5), 143.17 (C8), 120.74 (C9, C13), 131.21 (C10, C12), 137.22 (C11), 128.71 (C15), 131.81 (C16), 130.25 (C17), 154.16 (C18), 114.73 (C19), 134.83 (C20), 128.34 (C22), 131.28 (C23), 128.41 (C24), 155.21 (C25), 114.88 (C26), 132.66 (C27).

TABLE-5
UV-VIS SPECTRUM OF (MeFPT) LIGAND AS WELL AS ITS ORGANYLTELLURIUM(IV) COMPLEXES

Compound	λ_{max} (π-π^*) nm	λ_{max} (n-π^*) nm	λ_{max} (CT) nm
MeFPT	229	292	424
1a	256	306	439
1b	237	301	452
1c	240	312	461
1d	238	306	457
1e	241	304	463
1f	238	302	460

TABLE-6
SPECIFIED BOND ANGLES OF COMPLEX **1a**

Atom connectivity	Bond angles (°)	Atom connectivity	Bond angles (°)
C-Te-N	98.9873	C-Te-Cl	91.6171
N-Te-Cl	179.6565	Cl-Te-Cl	88.6936
N-Te-Cl	90.9635	O-Te-Cl	98.4723
O-Te-N	81.5355	Cl-Te-Cl	91.1434
N-Te-Cl	89.2000	O-Te-Cl	88.1143
C-Te-Cl	80.9962	Cl-Te-Cl	177.8643
C-Te-Cl	90.4607	O-Te-Cl	89.8036
C-Te-O	178.4917	–	–

TABLE-7
SPECIFIED BOND LENGTH OF LIGAND AND ITS COMPLEXES **1a** AND **1d**

Compound	C=N	C-O	Te-O	Te-N
MeFPT	1.29002	1.31432	–	–
1a	1.29914	1.29728	2.02335	2.10871
1d	1.29483	1.30207	2.05022	2.11167

Molecular modelling: With the help of Avogadro 4.0 version, the geometry optimization was carried out. The optimized structures of compounds are shown in Fig. 4. The data obtained are listed in Tables 6 and 7 where the bond angle and bond length of ligand and complexes (**1a** and **1d**) are compared. Furthermore, the data obtained concludes that bond angle values are indicating the octahedral geometry of synthesized complexes confirming the suggested structures. The bond

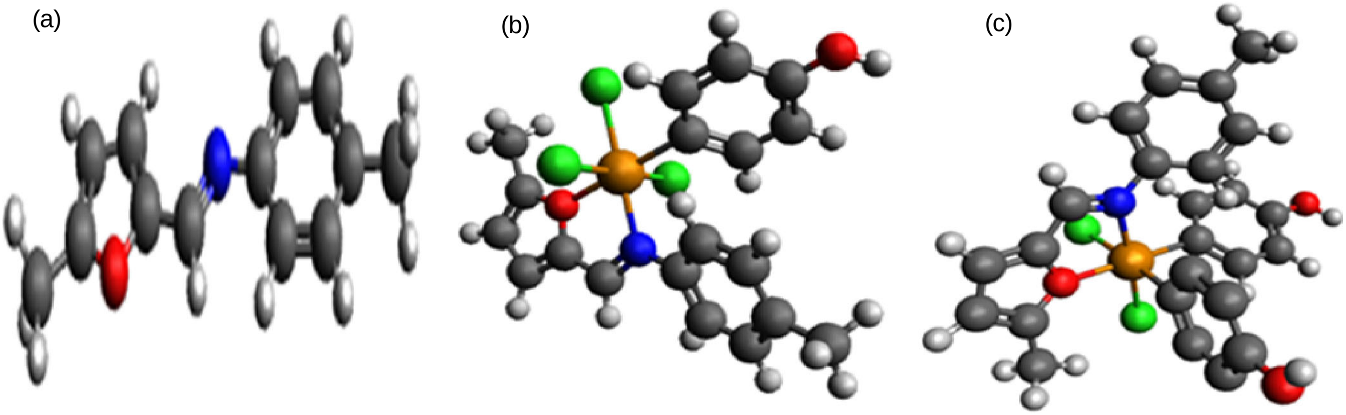

Fig. 4. Optimized structure of (a) MeFPT, (b) **1a** and (c) **1d**

length of azomethine (C=N) in ligand (MeFPT) is 1.29002 Å which becomes longer in the complexes indicating the coordination *via* N atom of azomethine similarly the change in C-O bond length values also shows coordination of O atom of furan ring to metal.

DFT study: The energy difference of FMO's (Frontier molecular orbitals) determines the electrical properties, reactivity and the stability of any compound. The highest occupied molecular orbitals (HOMO) and the lowest unoccupied molecular orbitals (LUMO) have a tendency to behave as electron donors and electron acceptors, respectively. The electronic transitions that take place from HOMO to LUMO of ligand and its metal complexes (**1a** and **1d**) illustrated in Fig. 5 was carried out by using program Avogadro 4.0 version with ORCA program. The energy values of HOMO and LUMO were used to calculate global reactivity descriptors such as hardness (η), electronegativity (χ), electrophilicity index (ω), softness (S), chemical potential (Pi) and are listed in Table-8.

TABLE-8
THEORETICAL DETERMINED QUANTUM PARAMETERS OF MeFPT, **1a** AND **1d**

Parameters	MeFPT	**1a**	**1d**
E_{HOMO} (eV)	-7.313	-6.342	-5.237
E_{LUMO} (eV)	-2.022	-1.338	-0.397
ΔE (eV)	-5.291	-5.004	-4.840
IE (eV)	7.313	6.342	5.237
X (eV)	4.667	3.840	2.817
η (eV)	2.645	2.502	2.420
S $(eV)^{-1}$	0.189	0.199	0.206
ω (eV)	4.117	2.940	1.639
Pi	-4.667	-3.840	-2.817

Antimicrobial activity: Antimicrobial activity of MeFPT ligand and its organyltellurium(IV) based complexes were investigated against Gram-positive and Gram-negative bacterial strains (*S. pyogenus*, *E. coli*, *S. aureus* and *P. aeruginosa*) and fungal strains (*A. niger*, *C. albicans* and *A. alavatus*). Table-9 shows the minimum inhibition concentration values for the ligand as well as its organyltellurium(IV) complexes. Ampicillin and greseofulvin were used as standard drugs. It is evident from Table-9 that the biological activities of tellurium(IV) complexes is enhanced as compared with free ligand. This can be justified taken into account the leading factors. One of the factor is chelate effect, *i.e.* complexes show higher antimicrobial efficiency rather than Schiff base ligand due to chelation and other factors are size of metal atom, coordination sites, nature of ligand *etc.* All the complexes (**1a-f**) shows striking antibacterial activity relative to the ligand. Among of all the complexes of tellurium, **1a** and **1e** exhibit excellent antibacterial activity against all the antibacterial strains. Complexes **1a**, **1b** and **1f** exhibit valuable antifungal activity, whereas **1b** show good antifungal activity against all the fungal species. Complex **1a** is the most effective besides all the complexes.

Conclusion

In this work, six organyltellurium(IV) complexes (**1a-f**) of type MeFPT·$RTeCl_3$ or MeFPT·R_2TeCl_2 have been synthesized when reacting Schiff base (MeFPT) with $RTeCl_3$ and R_2TeCl_2. Newly synthesized compounds were characterized by molar conductance, DFT, UV-vis, FT-IR, ^{1}H NMR, ^{13}C NMR and elemental analysis. Through the O atom of furan moiety and azomethine nitrogen, the Schiff base ligand acts as a bidentate ligand in all of the metal complexes. The distorted octahedral

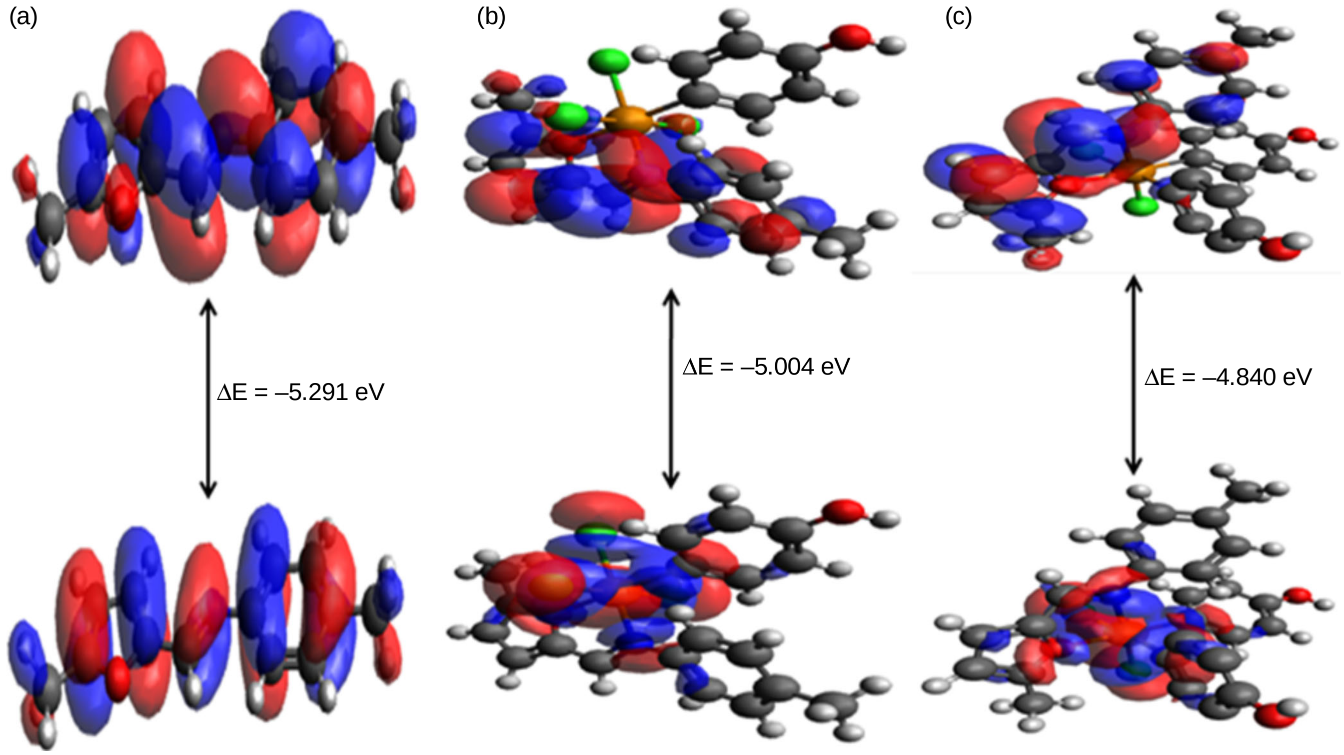

Fig. 5. HOMO and LUMO with (a) MeFPT energy gap, (b) **1a** energy gap (c) **1d** energy gap

TABLE-9
ANTIBACTERIAL AND ANTIFUNGAL ACTIVITIES OF (MeFPT) LIGAND AND ITS ORGANYLTELLURIUM(IV) COMPLEXES

Compounds	Antibacterial activity				Antifungal activity		
	S. aureus	*S. pyogenes*	*E. coli*	*P. aeruginosa*	*C. albicans*	*A. niger*	*A. clavatus*
L	0.25	0.5	0.5	0.2	0.5	0.5	1.0
1a	0.1	0.0625	0.0625	0.1	0.2	0.5	0.5
1b	0.5	0.2	0.5	0.5	0.1	0.1	0.1
1c	0.2	0.125	0.125	0.25	0.5	0.25	0.25
1d	0.2	0.5	0.5	1.0	0.5	0.25	0.25
1e	0.5	0.1	0.0625	0.1	0.5	0.5	0.5
1f	0.2	0.2	0.1	0.2	0.2	0.125	0.1
Ampicillin	0.25	0.1	0.1	0.1	–	–	–
Greseofulvin	–	–	–	–	0.5	0.1	0.1

geometry for these organyltellurium(IV) complexes has been proposed based on multiple spectroscopy approaches. These complexes outperform Schiff base ligand in antibacterial activity against many strains.

ACKNOWLEDGEMENTS

One of the authors, NA is grateful to Maharshi Dayanand University for providing University Research Scholarship and essential research resources. The authors also acknowledge SAIF, Punjab University, for CHN analysis, Guru Jambeshwar University for NMR and Mass spectral research and Microcare Laboratory, Surat, India for the antimicrobial activity.

CONFLICT OF INTEREST

The authors declare that there is no conflict of interests regarding the publication of this article.

REFERENCES

1. B. Naureen, G.A. Miana, K. Shahid, M. Asghar, S. Tanveer and A. Sarwar, *J. Mol. Struct.*, **1231**, 129946 (2021); https://doi.org/10.1016/j.molstruc.2021.129946
2. S. Kumar, D.N. Dhar and P. Saxena, *J. Sci. Ind. Res. (India)*, **68**, 181 (2009).
3. I.P. Ejidike and P.A. Ajibade, *Molecules*, **20**, 9788 (2015); https://doi.org/10.3390/molecules20069788
4. A.M. Abu-Dief and I.M.A. Mohamed, *Beni. Suef Univ. J. Basic Appl. Sci.*, **4**, 119 (2015); https://doi.org/10.1016/j.bjbas.2015.05.004
5. S. Mandal, T.K. Karmakar, A. Ghosh, M. Fleck and D. Bandyopadhyay, *Polyhedron*, **30**, 790 (2011); https://doi.org/10.1016/j.poly.2010.12.012
6. G. Ceyhan, C. Celik, S. Urus, I. Demirtas, M. Elmastas and M. Tümer, *Spectrochim. Acta A Mol. Biomol. Spectrosc.*, **81**, 184 (2011); https://doi.org/10.1016/j.saa.2011.05.106
7. J. Ceramella, D. Iacopetta, A. Catalano, F. Cirillo, R. Lappano and M.S. Sinicropi, *Antibiotics*, **11**, 191 (2022); https://doi.org/10.3390/antibiotics11020191
8. G.B. Bagihalli, P.G. Avaji, S.A. Patil and P.S. Badami, *Eur. J. Med. Chem.*, **43**, 2639 (2008); https://doi.org/10.1016/j.ejmech.2008.02.013
9. R. Pignatello, A. Panico, P. Mazzone, M.R. Pinizzotto, A. Garozzo and P.M. Fumeri, *Eur. J. Med. Chem.*, **29**, 781 (1994); https://doi.org/10.1016/0223-5234(94)90137-6
10. G.Y. Nagesh, K. Mahendra Raj and B.H.M. Mruthyunjayaswamy, *J. Mol. Struct.*, **1079**, 423 (2015); https://doi.org/10.1016/j.molstruc.2014.09.013
11. M. Salehi, A. Amoozadeh, A. Salamatmanesh, M. Kubicki, G. Dutkiewicz, S. Samiee and A. Khaleghian, *J. Mol. Struct.*, **1091**, 81 (2015); https://doi.org/10.1016/j.molstruc.2015.02.060
12. M.-F. Zaltariov, M. Cazacu, M. Avadanei, S. Shova, M. Balan, N. Vornicu, A. Vlad, A. Dobrov and C.-D. Varganici, *Polyhedron*, **100**, 121 (2015); https://doi.org/10.1016/j.poly.2015.07.030
13. E.M. Zayed and M.A. Zayed, *Spectrochim. Acta A Mol. Biomol. Spectrosc.*, **143**, 81 (2015); https://doi.org/10.1016/j.saa.2015.02.024
14. Z.Y. Sun, R. Yuan, Y.Q. Chai, L. Xu, X.X. Gan and W.J. Xu, *Anal. Bioanal. Chem.*, **378**, 490 (2004); https://doi.org/10.1007/s00216-003-2301-7
15. M. Valcarcal and M.D. Laque de Castro, Flow through Biochemical Sensors, Elsevier: Amsterdam (1976).
16. U. Spichiger-Keller, Chemical Sensor and Biosensor for Medical and Biological Application, Wiley-VCH: Weinheim (1998).
17. J.F. Lawrence and R.W. Frei, Chemical Derivation in Chromatography, Elsevier: Amsterdam (1976).
18. S. Menati, A. Azadbakht, R. Azadbakht, A. Taeb and A. Kakanejadifard, *Dyes Pigments*, **98**, 499 (2013); https://doi.org/10.1016/j.dyepig.2013.04.009
19. P. Singh, R. Goel and B. Singh, *J. Indian Chem. Soc.*, **52**, 958 (1975).
20. A. Datta, S. Walia and B.S. Parmar, *J. Agric. Food Chem.*, **49**, 4726 (2001); https://doi.org/10.1021/jf001318d
21. S. Basak, S. Sen, S. Banerjee, S. Mitra, G. Rosair and M.T.G. Rodriguez, *Polyhedron*, **26**, 5104 (2007); https://doi.org/10.1016/j.poly.2007.07.025
22. M. Irfan, R. Rehman, M.R. Razali, Shafiq-Ur-Rehman, Ateeq-Ur-Rehman and M.A. Iqbal, *Rev. Inorg. Chem.*, **40**, 193 (2020); https://doi.org/10.1515/revic-2020-0006
23. A.K. Singh, P.K. Raghavendra, G. Singh and S. Bali, *Phosphorus, Sulfur, Silicon Rel. Elem.*, **180**, 903 (2005); https://doi.org/10.1080/10426500590906409
24. S. Deepak Chouhan, K.K. Verma and S. Garg, *Int. J. Chem. Sci.*, **15**, 182 (2017).
25. A. Malik, G. Goyat and M. Vikas, *Chem. Sci. Trans.*, **7**, 374 (2018).
26. A. Malik, G. Goyat and K.K. Vikas, *Chem. Sci. Trans.*, **7**, 329 (2018).
27. A.I. Vogel, Practical Organic Chemistry, Including Qualitative Organic Analysis, Longmans, Green and Co.: London, New York, Toronto, Ed. 3, vol. 1188, p. 300 (1956).
28. A. Weissberger, Technique of Organic Chemistry, Interscience Publishers Inc.: New York, vol. 7 (1955).
29. N.N. Greenwood, B. Straughan and A.E. Wilson, *J. Chem. Soc. A: Inorg., Phys. Theor.*, **4**, 2209 (1968); https://doi.org/10.1039/j19680002209
30. W.J. Geary, *Coord. Chem. Rev.*, **7**, 81 (1971); https://doi.org/10.1016/S0010-8545(00)80009-0
31. A. Apelblat, *J. Solution Chem.*, **40**, 1234 (2011); https://doi.org/10.1007/s10953-011-9718-y
32. A. Kakanejadifard, F. Esna-ashari, P. Hashemi and A. Zabardasti, *Spectrochim. Acta A Mol. Biomol. Spectrosc.*, **106**, 80 (2013); https://doi.org/10.1016/j.saa.2012.12.044
33. A. Trzesowska-Kruszynska, *J. Mol. Struct.*, **1017**, 72 (2012); https://doi.org/10.1016/j.molstruc.2012.03.003
34. Deepak, S. Chouhan, K.K. Verma and S. Garg, *Chem. Sci. Trans.*, **6**, 448 (2017).

35. G. Goyat, S. Garg and K.K. Verma, *Chem. Sci. Trans.*, **5**, 479 (2016).
36. Deepak, S. Chouhan, K.K. Verma and S. Garg, *Int. J. Chem. Sci.*, **14**, 269 (2016).
37. M. Shakir, A. Abbasi, A.U. Khan and S.N. Khan, *Spectrochim. Acta A Mol. Biomol. Spectrosc.*, **78**, 29 (2011); https://doi.org/10.1016/j.saa.2010.02.034
38. A. Pui, T. Malutan, L. Tataru, C. Malutan, D. Humelnicu and G. Carja, *Polyhedron*, **30**, 2127 (2011); https://doi.org/10.1016/j.poly.2011.05.029
39. G. Goyat, A. Malik, S. Garg and K.K. Verma, *Int. J. Chem. Sci.*, **14**, 387 (2016).
40. G. Goyat, A. Malik, S. Garg and K.K. Verma, *Int. J. Chem. Sci.*, **14**, 1498 (2016).
41. G. Goyat, S. Garg and K.K. Verma, *Res. J. Pharm. Biol. Chem. Sci.*, **7**, 869 (2016).
42. M. Kumar, P.J. Darolia, S. Chauhan, M. Sindhu, K.K. Verma and S. Garg, *ChemistrySelect*, **6**, 5778 (2021); https://doi.org/10.1002/slct.202101184
43. G.G. Mohamed, M.M. Omar and A.M. Hindy, *Turk. J. Chem.*, **30**, 361 (2006).
44. O.M. Ali, *Spectrochim. Acta A Mol. Biomol. Spectrosc.*, **132**, 52 (2014); https://doi.org/10.1016/j.saa.2014.03.127
45. A.A. Abdel-Aziz, A.N. Salem, M.A. Sayed and M.M. Aboaly, *J. Mol. Struct.*, **1010**, 130 (2012); https://doi.org/10.1016/j.molstruc.2011.11.043
46. M.M. Aboaly and M.M.H. Khalil, *Spectrosc. Lett.*, **34**, 495 (2001); https://doi.org/10.1081/SL-100105095
47. D. Dey, G. Kaur, A. Ranjani, L. Gayathri, P. Chakraborty, J. Adhikary, J. Pasan, D. Dhanasekaran, A.R. Choudhury, M.A. Akbarsha, N. Kole and B. Biswas, *Eur. J. Inorg. Chem.*, 3350 (2014); https://doi.org/10.1002/ejic.201402158